

Generation and manipulation of monodispersed ferrofluid emulsions: the effect of an uniform magnetic field in flow-focusing and T-junction configurations

Say Hwa Tan¹ and Nam-Trung Nguyen^{1, a)}

*School of Mechanical and Aerospace Engineering, Nanyang Technological University,
50 Nanyang Avenue, Singapore 639798, Singapore*

(Dated: 10 February 2011)

This paper demonstrates the use of magnetically controlled microfluidic devices to produce monodispersed ferrofluid emulsions. By applying a uniform magnetic field on flow-focusing and T-junction configurations, the size of the ferrofluid droplets can be actively controlled. The influences of the flow rates, the orientation and the polarity of the magnetic field on the size of ferrofluid droplets in flow-focusing and T-junction configurations are compared and discussed.

PACS numbers: 47.55.df, 75.50.Mm, 47.61.Fg, 47.55.dd, 47.61.Jd

Keywords: ferro fluid, droplet, capillary force, emulsion

^{a)}Electronic mail: mntnguyen@ntu.edu.sg

I. INTRODUCTION

Ferrofluid is a class of "smart" fluids¹ which have been extensively used in a number of applications. Ferrofluids possessed attractive properties such as easy magnetization and demagnetization, maintaining its fluidity even when subjected to a strong magnetic field², high rates of heat transfer³ and changes of viscosity in moderate magnetic fields⁴. These properties make ferrofluids very useful for engineering and biomedical applications. Engineering applications include cooling of loudspeakers⁵, magnetic sealing in bearings⁶, accelerometers⁷ and tilt sensors for underground pipes⁸. In medical fields, ferrofluids are attractive drug carriers due to their intrinsic physical properties and their abilities to target specific locations which thereby minimizing severe side effects. Common clinical applications includes magnetic drug targeting⁹, treatment of thrombosis¹⁰ and tumor therapy¹¹. Theoretical studies of ferrofluids includes the well known normal field instability and pattern formation¹², particles chain aggregation¹³ and structural transitions in different magnetic fields¹⁴.

Recently, ferrofluid emulsions have been attracting great interest from researchers due to its ability to discretize, isolate, react, compartmentalize and magnetically transport samples and reagents to targeted locations. These features are suitable for many lab-on-chip applications. Ferrofluid emulsions integrated with microfluidic devices have applications in areas such as production of magnetic particles¹⁵, polymerase chain reaction (PCR)¹⁶ and micropumps¹⁷. Conventional approach to produce ferrofluid emulsions involves vigorous mixing of the ferrofluid with another immiscible fluid, applying several purifications steps and repeated pipetting to obtain highly monodispersed ferrofluid emulsions¹⁸. Another approach to produce submicron ferrofluid emulsions involves the use of a coquette mixer to shear the emulsions and subsequent sorting under a magnetic field to collect the narrowly size-distributed emulsions¹⁵. Both methods are often tedious, laborious and time consuming. Understanding these predicaments, this paper presents a simple approach to produce highly monodispersed ferrofluid emulsions by using simple microfluidic devices.

In our previous work, we demonstrated a novel way to control the production and manipulate the size of ferrofluid emulsions using a permanent magnet integrated into a microfluidic T-junction geometry¹⁹. However, this method does not allow controllable manipulation as it requires the permanent magnet to be placed at different locations. Several restrictions such as magnet strength and size also limits the manipulation process. Knowing these limitations,

in this current work, water-in-oil ferrofluid emulsions are produced in both microfluidic T-junction and flow-focusing configurations and then compared. These highly monodispersed ferrofluid emulsions can be first generated and then also collected for further use. Besides using conventional flow rates, this paper presents a robust and active mean to control the size of the ferrofluid emulsions. By applying a uniform magnetic field across the microfluidic devices, the size of the ferrofluid droplets produced can hence be actively manipulated at ease using magnetic field which in turn is controlled by the applied electric current of an electromagnet. The effect of a uniform magnetic field in the different configurations and the polarity of the magnetic field are also presented and discussed.

II. EXPERIMENTAL

A. Device Fabrication

The microfluidic devices were fabricated using standard soft lithography²⁰. First, a layout editor (Clewin, The Netherlands) was used to design the the devices. Each microfluidic device has a total area of only 1 cm by 1 cm. The schematic sketch and dimensions of both flow-focusing and T-junction configurations used in the experiments are shown in Figure 1. Next, a master mold was fabricated using the negative SU-8 photoresist (MicroChem SU8-2100, USA). The thickness of the mold which defines the rectangular channel depth is 100 μm thick. PDMS oligomer and crosslinking prepolymer is mixed in the ratio of 10:1 and placed in a vacuum desiccator for 1 hour for degassing. The degassed PDMS mixture is then poured onto the master mold and cured in a convection oven for 2 hours. After curing, the casted PDMS was peeled from the SU-8 mold and punched using a manual puncher (Harris Uni-Core, World Precision Instruments, USA). Fluidic access holes with a diameter of 1.2 mm were created. The casted PDMS was then soaked in Isopropanol (IPA) for 15 minutes followed by rinsing in distilled (DI) water. The cleaning step prevents dirt and dust from accumulating on the PDMS cast. After the cleaning process, the PDMS parts were dried using nitrogen gas at high pressure to ensure that no dusts reside on the surface of the PDMS cast which may later affect the bonding integrity. The PDMS cast was then placed in an oven at 150°C for 30 minutes to ensure that the surface is free of water. Lastly, oxygen plasma treatment (NT-2, BSET EQ) at 120 W for 45 seconds was used to bond the device

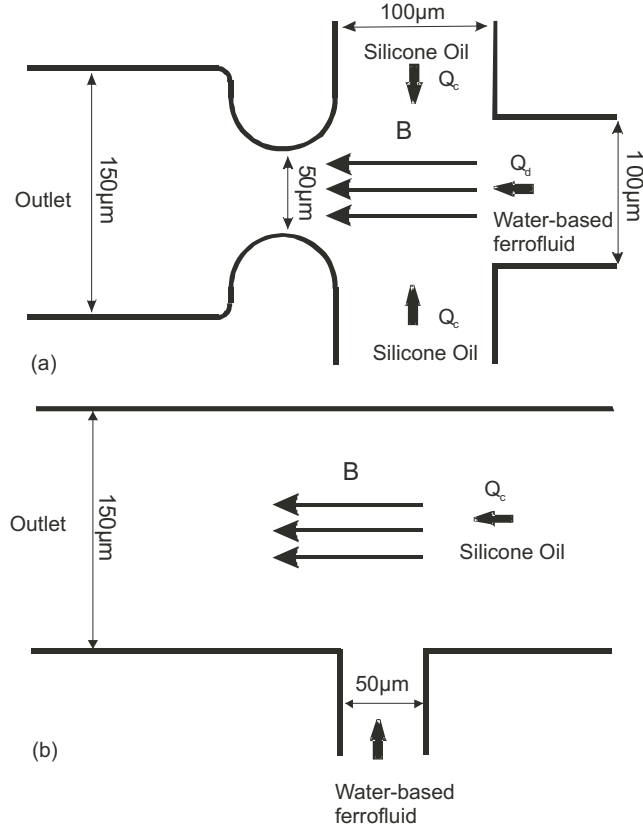


FIG. 1. Schematic sketch of the microfluidic geometries used (not drawn to scale): (a) Flow focusing and (b) T-junction.

to a 200- μm layer PDMS spin-coated on a glass slide. The fabrication process is summarized in Figure 2.

B. Materials

In order to produce ferrofluid emulsions, two immiscible fluids were introduced into the inlet channels of the devices. Silicone oil (378364, Sigma-Aldrich) with a dynamic viscosity of 96 mPa.s and density of 960 kg.m^{-3} works as the continuous phase (CP). Water based ferrofluid (EMG707, Ferrotec) with a dynamic viscosity of 5 mPa.s and density of 1100 kg.m^{-3} works as the dispersed phase (DP). The ferrofluids contains spherical Fe_3O_4 magnetic nano particles which have an average diameter of 10 nm. As the size of the magnetic nanoparticles are very small, weak or negligible magnetoviscous effect is expected⁵. The volume concentration of the magnetic nanoparticles is 1.8% and its initial susceptibility is 0.36. The saturation magnetization of the ferrofluid is about 10 mT and the dielectric number is about

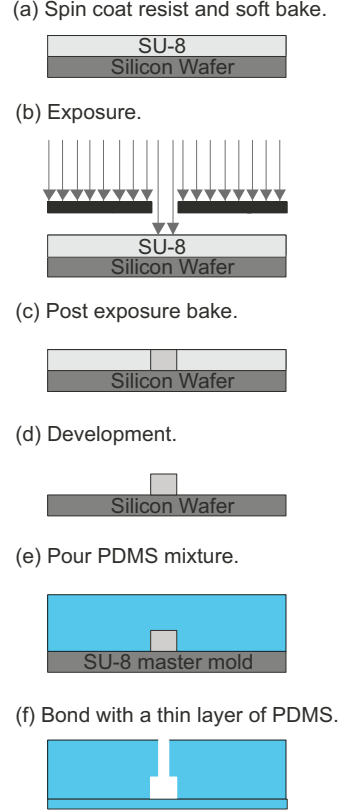


FIG. 2. Fabrication process of the microfluidic device: (a)-(d) Fabrication of SU-8 master mold and (e)-(f) is the fabrication of PDMS.

75. The magnetic nanoparticles are coated with an unknown anionic surfactants which serve as a protective layer²¹ and prevents particles aggregation²². The interfacial tension between the ferrofluid and silicone oil was measured using a commercial tensiometer (TVT-2, Lauda) and is approximately 33 mN.m²³.

C. Experiment setup and procedure

The schematic sketch of the experimental setup is shown in Figure 3. First, the uniform magnetic field is generated using a coil with 350 turns assembled around a C-shape iron core²⁴. A separation gap of 26 mm ensures that the generated magnetic field is homogenous and uniform. Next, the microfluidic devices are positioned in the middle of the gap. For the flow-focusing device, the channel of the dispersed phase is aligned parallel to the magnetic field. For the T-junction device, the channel of the dispersed phase is aligned perpendicular to magnetic field. During the formation process of the emulsion, the direction of the magnetic

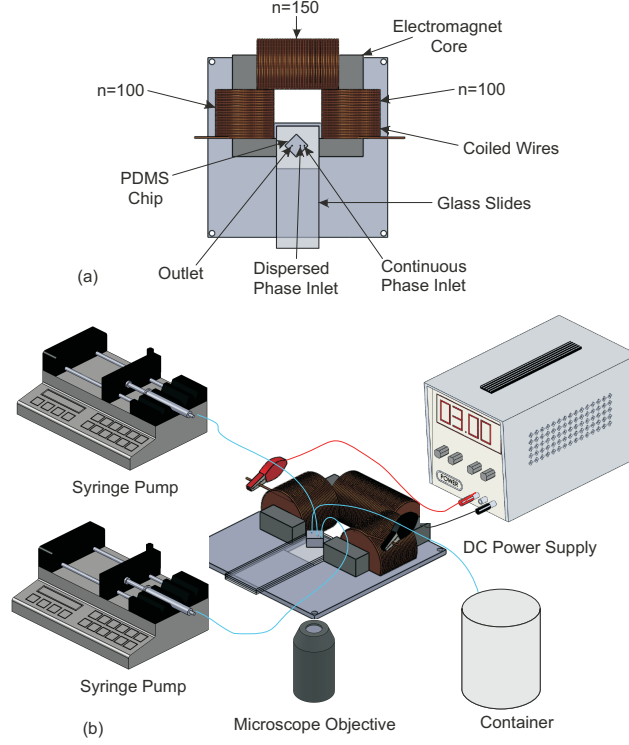


FIG. 3. Schematic sketch of the experimental setup (not drawn to scale): (a) Top view and details of the electromagnet and (b) experimental setup.

field is parallel to the fluid motion in both cases to ensure a fair comparison. Figure 4 shows the measured magnetic field strength at different position relative to the midpoint of the dispersed phase channel in the microfluidic devices. The result shows and confirms the uniformity of the magnetic field within the region of emulsion formation. A first order fit for the measured values depicts a linear straight line with negligible gradient. The magnetic flux densities were measured using a commercial gaussmeter (Hirst GM05, UK) with an accuracy of $\pm 1\%$. A DC power source (GPS-3030DD, Instek) was used to vary the magnitudes of the magnetic flux density by changing the applied electric current. An inverted microscope (TE 2000, Nikon) and a high-speed camera (APX RS, Photron) were used to capture the droplet formation process. Two syringe pumps (KDS 250, KDS Scientific) were used to deliver the fluids into the microfluidic devices at fixed flow rates separately.

The experiments were conducted by fixing the flow rates of both the dispersed and continuous phases and varying the magnetic flux density. Three different sets of flow rates with the same flow rate ratio were tested in the experiments. As silicone oil results in slight swelling of PDMS²³, the fluids were allowed to flow for 20 minutes before the collection of

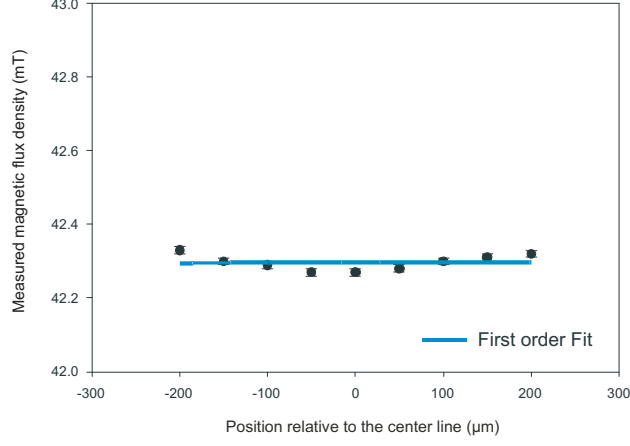


FIG. 4. Measured magnetic flux density as a function of relative position to the centre line. The magnetic field is generated using a constant current of 3 A. The centre line represents the midpoint in the dispersed phase channel. A positive distance indicates the upstream and a negative position indicates the downstream position. The position is adjusted using a micropositioner.

the images. This measure minimized the structural change within the microfluidic devices. Images of the formation process were acquired at a rate of 1000 frames per second. The size of the ferrofluid emulsions produced were then evaluated using a customized image processing software (MATLAB, MathWorks). The magnetic flux density of the electromagnet is varied by changing the supplied current at a regular intervals of 0.5 A. A stabilization time of 15 minutes was also used at each interval.

III. RESULTS AND DISCUSSIONS

A. Flow-Focusing Configuration

Figure 5(a) shows the diameter of the ferrofluid droplets formed as a function of magnetic flux density in the flow-focusing geometry. In the absence of the magnetic field, the ferrofluid emulsions are formed in the “geometry-controlled/squeezing” regime²⁵. The ferrofluid emulsions produced in this regime are highly monodispersed. In each ferrofluid droplet formation process, the “finger” of the dispersed fluid progresses sequentially into the orifice. As the ferrofluid tip advances, it first increases in size and then evolves into a conical shape. This process limits the flow of the outer fluids and thus results in the change in shape for the dispersed finger. As the dispersed finger blocks the flow of the outer fluids, the downstream

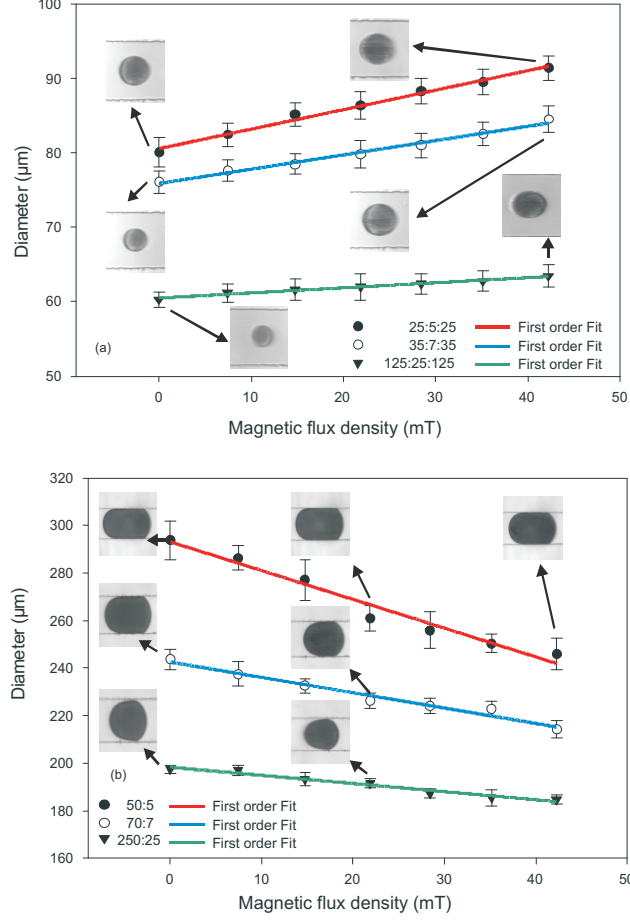


FIG. 5. Size of ferrofluid emulsions as a function of magnetic flux density. (a) Flow-focusing configuration and (b) T-junction configuration.

pressure builds up gradually. The dispersed finger is elongated and changes the curvature of the neck²⁶. Thinning of the neck occurs as the downstream pressure increases. A ferrofluid droplet is formed when the capillary pressure balances with the viscous forces which then "pinches" off the dispersed neck to form the droplet. After the formation, the dispersed "finger" retracts to its original position located upstream and returns back to its domical shape. At a fixed flow rate ratio (CP:DP:CP = 5:1:5). The size of the droplet decreases with the increase of total flow rates [Figure 5(a)] due to the higher shear rate at higher total flow rates and the less dominant capillary pressure. At a higher total flow rate, the shape of the dispersed "finger" becomes more conical due to the higher shearing force imposed by the continuous phase. The trends observed throughout the experiments agree with the scaling argument proposed by Garstecki et al.²⁶.

In the presence of a magnetic field, the size of the ferrofluid droplets produced changes

with the applied magnetic flux density. In general, the size increases with the increase of the magnetic flux density, Figure 5(a). As the dispersed phase fluid is aligned in the direction of the magnetic field, the magnetic nano particles in the dispersed phase aligns and orients itself in the direction of the magnetic field³. The the additional magnetic force stretches the fluid finger and induces internal secondary flow. The elongation of the finger delays the thinning process of the neck and consequently the breakup of the droplet. Details of the effect of the magnetic field on the formation process in a flow-focusing configuration were investigated numerically by our group. In addition, others factors such as the local change of magnetic induced changes to the local viscosity²⁷ and changes in interfacial slips due to the presence of the nanoparticles may also contributes to the changes. Figure 6 depicts the movement of the magnetic nanoparticles along the magnetic field within the dispersed phase²⁸. The experimental results also suggested that these changes are affected by the total flow rate. At a higher total flow rate, the change in size of the ferrofluid emulsions at a stronger magnetic field is less prominent and significant. At a higher total flow rate, the dependence on the change in dispersed fluid flow rates is smaller. The first order fits obtained in the experimental results also shows a decrease in gradient at higher total flow rates.

B. T-junction Configuration

Figure 5(b) shows the diameter of ferrofluid droplets as a function of magnetic flux density at the T-junction configuration. In the absence of the magnetic field, the ferrofluid droplets are formed in the same "geometry controlled/squeezing" regime. However under the same flow rates, the sizes of the ferrofluid droplets formed were bigger than the one formed in the flow-focusing configuration, because the dispersed phase fluid is not confined by the orifice²⁵ which limits the size of the droplets. In the T-junction geometry, the confinement of the dispersed phase fluid is smaller due to a larger separation distance between the channel of the dispersed phase and the channel of the continuous phase. The size of the orifice in the flow-focusing geometry is about 50 μm and the size of the separation distance in the T-junction is about 150 μm . The emulsions formation process in the T-junction is also different as compared to the flow-focusing configuration. In the T-junction configuration, the ferrofluid droplets are formed via a two-stage growth process^{29,30}. First, the dispersed

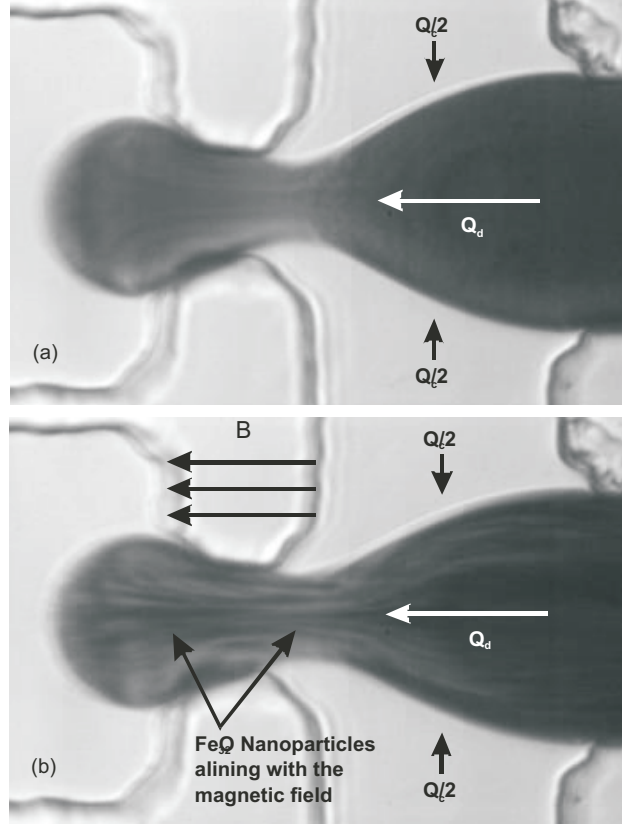


FIG. 6. Alignments of the magnetic nanoparticles in the direction of the magnetic field. In both cases, the flow rates are fixed at 25:5:25 (CP:DP:CP). (a) Without magnetic field and (b) at magnetic flux density of 42.3 mT.

phase fluid gradually extrudes into the continuous phase channel and occupies the full width of the continuous phase channel. The obstruction cause by the dispersed fluid also blocks the flow of the continuous-phase fluid which increases the upstream pressure. The emulsion then grows in size, while simultaneously reduces the neck of the dispersed phase. The upstream pressure then pinches off the dispersed neck and formed the emulsion when the dispersed phase fluid cannot withstand the upstream pressure. At a fixed flow rate ratio (CP:DP = 10:1), the sizes of the emulsions produced also changes with the change in total flow rate. A smaller ferrofluid emulsion is formed when the total flow rate increase, due to the higher shear rate and lower dependence of capillary pressure at higher flow rates. Compared to the flow-focusing configuration, the change in total flow rates for the T-junction configuration has a greater effect on the size of the formed ferrofluid droplets. A greater change in the size of the droplet size is observed when the total flow rate increases.

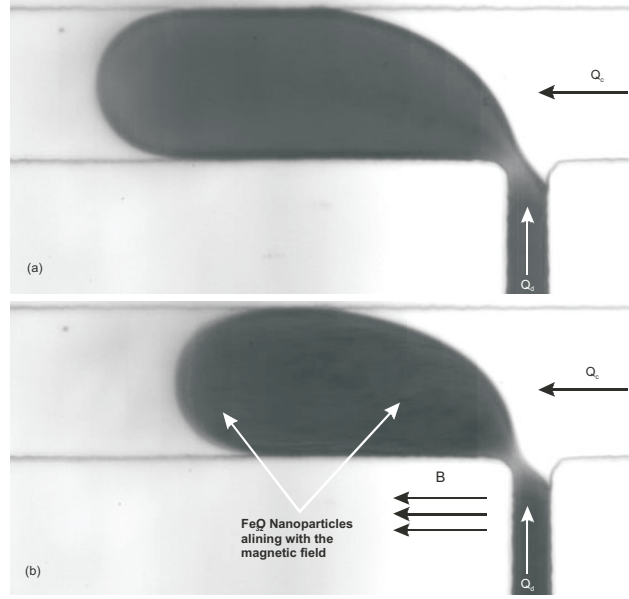


FIG. 7. Alignments of the magnetic nanoparticles in the direction of the magnetic field. In both cases, the flow rates are fixed at 50:10 (CP:DP). (a) Without magnetic field and (b) at magnetic flux density of 42.3 mT.

In the presence of a magnetic field, the size of the ferrofluid droplets also changes with the applied magnetic flux density. However, in contrast to the flow-focusing geometry, the size of the ferrofluid emulsions produced at the T-junction decreases with the increase of the magnetic flux density. This difference in behavior is mainly caused by the orientation of the magnetic field relative to the flow of the ferrofluid. In the flow focusing configuration, the elongation delays the breakup. However, in the T-junction configuration, the extruding dispersed phase fluid is perpendicular to the orientation of the magnetic field. The elongation accelerates the thinning process of the neck and makes the droplet to break up earlier as compared to the case without the magnetic field. Figure 7 illustrates the alignments of the magnetic nanoparticles in the direction of the magnetic field in the T-junction configuration. At higher total flow rates, the change in size of the ferrofluid emulsions at higher magnetic flux density is also less prominent. This phenomenon is similar to the one observed in the flow focusing experiments.

C. Effect of magnetic polarity

In order to investigate the effect of the magnetic polarity on the size of ferrofluid emulsion produced, the experiments reported above were repeated with a change in the direction of the electrical current. This change in direction of the current induced a change in the polarity of the uniform magnetic field. Figure 8 shows the effect of the magnetic polarity in both flow-focusing and T-junction configurations. Suprisingly, when the direction of the magnetic field is reversed, the trends obtained for the size of the ferrofluid droplets are similar in all cases. This phenomenon suggests that the direction of the magnetic polarity has little or no obvious influence on the size of the ferrofluid emulsion produced in microfluidic devices. The magnetic polarity does not affect the size of the ferrofluid droplets.

IV. CONCLUSIONS

In this study, we introduced a novel method to produce and actively manipulate the size of the ferrofluid droplets produced using simple microfluidic devices. Unlike in our previous work, this method offers a flexible and reliable method to control the size of the ferrofluid emulsion produced using simple microfluidic devices. From the experimental results, the following conclusions can be drawn. First, the size of the ferrofluid emulsions formed was found to change with the change in the flow rates, orientation and the strength of the magnetic field. This demonstrates and ascertained that the concept can be used to effectively manipulate the size of the ferrofluid emulsions produced in microfluidic devices. Second, in the flow focusing configuration, the size of the ferrofluid emulsions produced increases with the increase in magnetic flux density, because the dispersed fluid is parallel to the direction of the magnetic fields. At higher flow rates, the effect is less prominent due to a lower dependence on the changes in the dispersed flow rate. Third, in the T-junction configuration, the size of the ferrofluid emulsions produced decreases with the increase in magnetic flux density, because the dispersed fluid is aligned perpendicularly to the magnetic field. The alignments of the magnetic nanoparticles with the magnetic field changes the interfacial slips of the dispersed fluid, affects the magnetic induced changes in local viscosity coefficients and thus results in the decrease in the size of the ferrofluid emulsions produced. At higher flow rates, the effect is less dominant. Fourth, the effect of the magnetic polarity

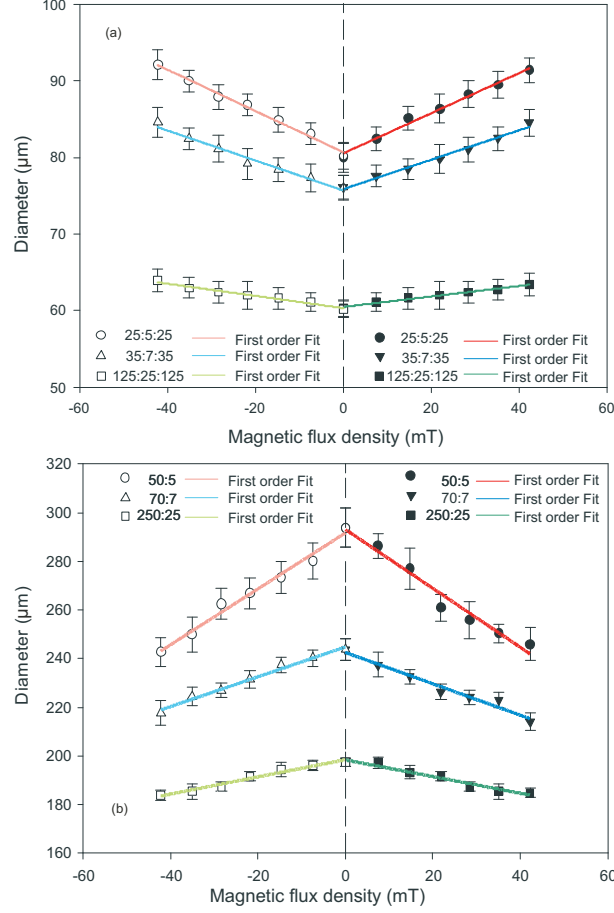


FIG. 8. Effect of the polarity of the magnetic field. Each colored line represents different fixed flow rates used. The dark colored lines represent the ferrofluid emulsions formed using a positive magnetic flux density. The light colored lines represent the ferrofluid emulsion formed using a negative magnetic flux density. (a) Using the flow focusing geometry and (b) using the T-junction geometry.

was found to have no influence on the size of the ferrofluid droplets produced in both flow focusing and T-junction geometry, because the direction of the magnetic polarity does not change the alignments of the magnetic nanoparticles with the magnetic field. Lastly, this unique method proposed to actively manipulate size of the ferrofluid emulsions formed, may be a simple alternative adopted to solve multiple complex problems faced by many fellow researchers in different fields. This work also open up many exciting opportunities for researchers in the application of magnetic nanoparticles.

ACKNOWLEDGEMENT

We gratefully acknowledge the insightfully discussions held with Dr Jean-Christophe Baret from the Max-Planck Institute for Dynamics and Self-organization.

REFERENCES

- ¹S. S. Nair, J. Thomas, C. S. Suchand Sandeep, M. R. Anantharaman, and R. Philip, Applied Physics Letters **92**, 171908 (2008).
- ²C. Scherer and A. M. Figueiredo Neto, Brazilian Journal of Physics **35**, 718 (2005).
- ³K. Raj and R. J. Boulton, Materials & Design **8**, 233 (1987).
- ⁴L. M. Pop, J. Hilljegerdes, S. Odenbach, and A. Wiedenmann, Applied Organometallic Chemistry **18**, 523 (2004).
- ⁵S. Odenbach, Colloids and Surfaces A: Physicochemical and Engineering Aspects **217**, 171 (2003).
- ⁶K. Raj and R. Moskowitz, Journal of Magnetism and Magnetic Materials **85**, 233 (1990).
- ⁷R. L. Bailey, Journal of Magnetism and Magnetic Materials **39**, 178 (1983).
- ⁸K. Raj, B. Moskowitz, and R. Casciari, Journal of Magnetism and Magnetic Materials **149**, 174 (1995).
- ⁹R. Ganguly, A. P. Gaind, S. Sen, and I. K. Puri, Journal of Magnetism and Magnetic Materials **289**, 331 (2005).
- ¹⁰A. N. Rusetski and E. K. Ruuge, Journal of Magnetism and Magnetic Materials **85**, 299 (1990).
- ¹¹A. S. Lübke, C. Alexiou, and C. Bergemann, Journal of Surgical Research **95**, 200 (2001).
- ¹²A. G. Boudouvis, J. L. Puchalla, L. E. Scriven, and R. E. Rosensweig, Journal of Magnetism and Magnetic Materials **65**, 307 (1987).
- ¹³V. S. Mendelev and A. O. Ivanov, Physical Review E - Statistical, Nonlinear, and Soft Matter Physics **70**, 051502 (2004).
- ¹⁴M. Ivey, J. Liu, Y. Zhu, and S. Cutillas, Physical Review E - Statistical, Nonlinear, and Soft Matter Physics **63**, 1 (2001).
- ¹⁵F. Montagne, O. Mondain-Monval, C. Pichot, H. Mozzanega, and A. Ellassari, Journal of Magnetism and Magnetic Materials **250**, 302 (2002).

- ¹⁶Y. Sun, Y. C. Kwok, and N. T. Nguyen, Lab on a Chip - Miniaturisation for Chemistry and Biology **7**, 1012 (2007).
- ¹⁷A. Hatch, A. E. Kamholz, G. Holman, P. Yager, and K. F. Böhringer, Journal of Microelectromechanical Systems **10**, 215 (2001).
- ¹⁸J. Bibette, Journal of Magnetism and Magnetic Materials **122**, 37 (1993).
- ¹⁹S. Tan, N. Nguyen, L. Yobas, and T. Gang, Journal of Micromechanics and Microengineering **20**, 045004 (2010).
- ²⁰D. C. Duffy, J. C. McDonald, O. J. A. Schueller, and G. M. Whitesides, Analytical Chemistry **70**, 2280 (1998).
- ²¹X. R. Qu, S. C. Lü, S. F. Fu, and Q. Y. Meng, Key Engineering Materials **428-429**, 533 (2010).
- ²²N. Pamme, Lab on a Chip - Miniaturisation for Chemistry and Biology **6**, 24 (2010).
- ²³M. He, J. Kuo, and D. Chiu, Langmuir **22**, 6408 (2006).
- ²⁴C. Ogawa, Y. Masubuchi, J. I. Takimoto, and K. Koyama, International Journal of Modern Physics B **15**, 859 (2001).
- ²⁵S. L. Anna and H. C. Mayer, Physics of Fluids **18**, 121512 (2006).
- ²⁶P. Garstecki, H. A. Stone, and G. M. Whitesides, Physical Review Letters **94**, 164501 (2005).
- ²⁷C. Flament, S. Lacis, J.-C. Bacri, A. Cebers, S. Neveu, and R. Perzynski, Physical Review E - Statistical Physics, Plasmas, Fluids, and Related Interdisciplinary Topics **53**, 4801 (1996).
- ²⁸S. M. S. Murshed, S. H. Tan, N. T. Nguyen, T. N. Wong, and L. Yobas, Microfluidics and Nanofluidics **6**, 253 (2009).
- ²⁹H. Liu and Y. Zhang, Journal of Applied Physics **106**, 034906 (2009).
- ³⁰M. De Menech, P. Garstecki, F. Jousse, and H. A. Stone, Journal of Fluid Mechanics **595**, 141 (2008).
- ³¹E. K. Ruuge and A. N. Rusetski, Journal of Magnetism and Magnetic Materials **122**, 335 (1993).
- ³²J. Liu, Y. F. Yap, and N. Nguyen, Physics of Fluids **under consideration**, xxx (2011).